Supplementary information

1 Influence of the relative quantities of $AgNO_3$, $NaBH_4$, and AA on the morphology of nanodisks

The concentration of AA has been varied, with all the other parameters set to the values of the standard protocol. The UV-visible spectra of the corresponding dispersions are reported in Fig. 1. Increasing the AA concentration decreases the aspect ratio of the nanodisks.

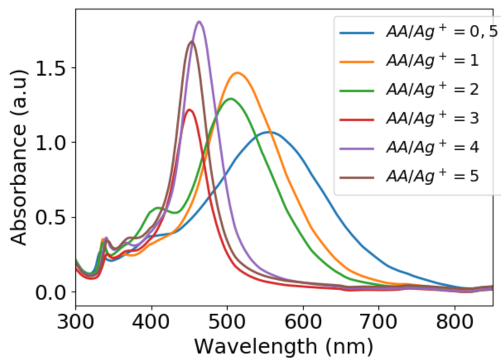

Figure 1: Effect of the variation of the AA concentration on the nanodisk morphology.

The concentration of NaBH4 has also been varied, with all the other parameters set to the values of the standard protocol. The UV-visible spectra of the corresponding dispersions are reported in Fig. 2. Increasing the NaBH4 concentration decreases the size of the nanodisks due to an increase of the number of available seeds.

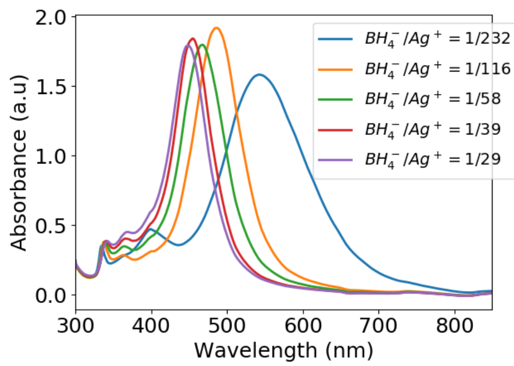

Figure 2: Effect of the variation of the NaBH4 concentration on the nanodisk morphology.

2 Syntheses with only one reducing agent

Syntheses were conducted with only ascorbic acid (weak reducer) or sodium borohydride (strong reducer) to show that using the two reducers simultaneously is necessary for obtaining anisotropic particles. The results of syntheses led with ascorbic acid only or $NaBH_4$ only are presented in Figs. 3 and 4, respectively.

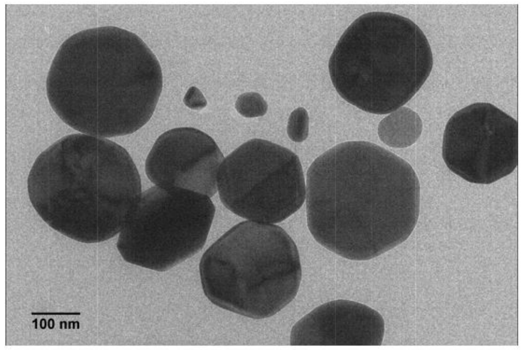

Figure 3: TEM image of silver nanoobjects synthesized using solely L-ascorbic acid and stabilized by PVP, Scale bar: 100 nm. There are no more plasmonic effects with these large particles : the suspension is only turbid.

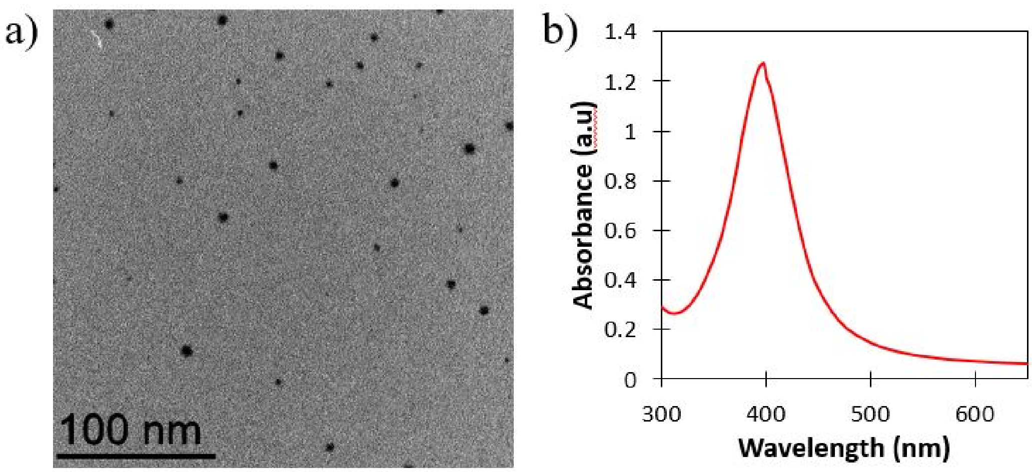

Figure 4: a) TEM image of an example of silver nanoobjects synthesized using solely $NaBH_4$ as reducing agent and stabilized by PVP, Scale bar: 100 nm; b) Corresponding UV-Visible spectra showing the typical band of these 3D silver nanoobjects.

3 DDA simulation of a single platelet decomposing in-plane and out-of-plane modes

DDA simulations have been conducted with prescribed light polarization and orientation of a nanodisk in order to isolate the in-plane and out-of-planes plasmon modes. The results reported in Fig. 5 show that the in-plane oscillation is responsible for the main low energy peak only and that the other two smaller peaks correspond dipolar and quadrupolar the out-of-plane modes.

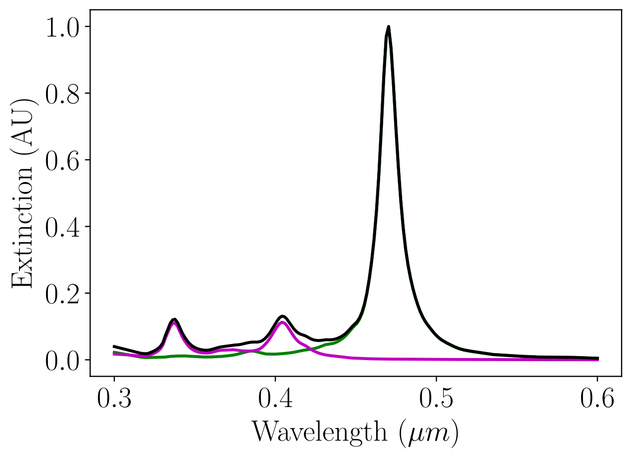

Figure 5: In-plane (green) and out-of-plane (magenta) spectra corresponding to pure in-plane and out-of-plane excitation with prescribed light polarization in DDA simulations. The black curve is the sum. The AgND considered is a cylinder of height 8 nm and diameter 22 nm.

4 In-situ-seeding syntheses conducted above or below room temperature.

The standard synthesis protocol described thoroughly in the article has been reproduced at $40°C$ and $10°C$. The corresponding characterizations of the resulting dispersions for $NaBH_4$ injection times ranging between 5 s and 120 s are reported in Figs. 6 and 7.

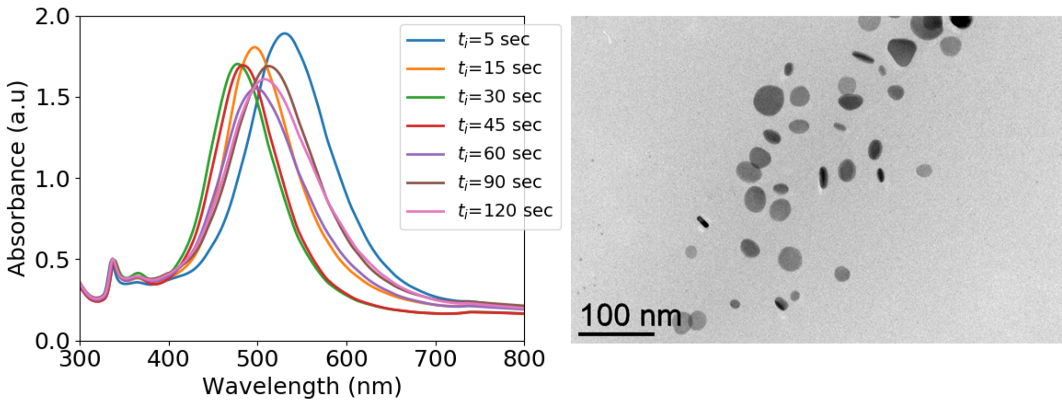

Figure 6: Influence of t_i on the synthesis at $40°C$.

5 Temperature dependence of the nucleation threshold.

A qualitative evaluation of the temperature dependence of the silver nanocrystals nucleation threshold has been carried out using only silver ions and $NaBH_4$. The silver ion concentration was set to 0.1733 mM and the concentration of reducer was varied. The pictures reported in Fig. 8 show that the nucleation threshold increases significantly in the temperature range investigated in the article.

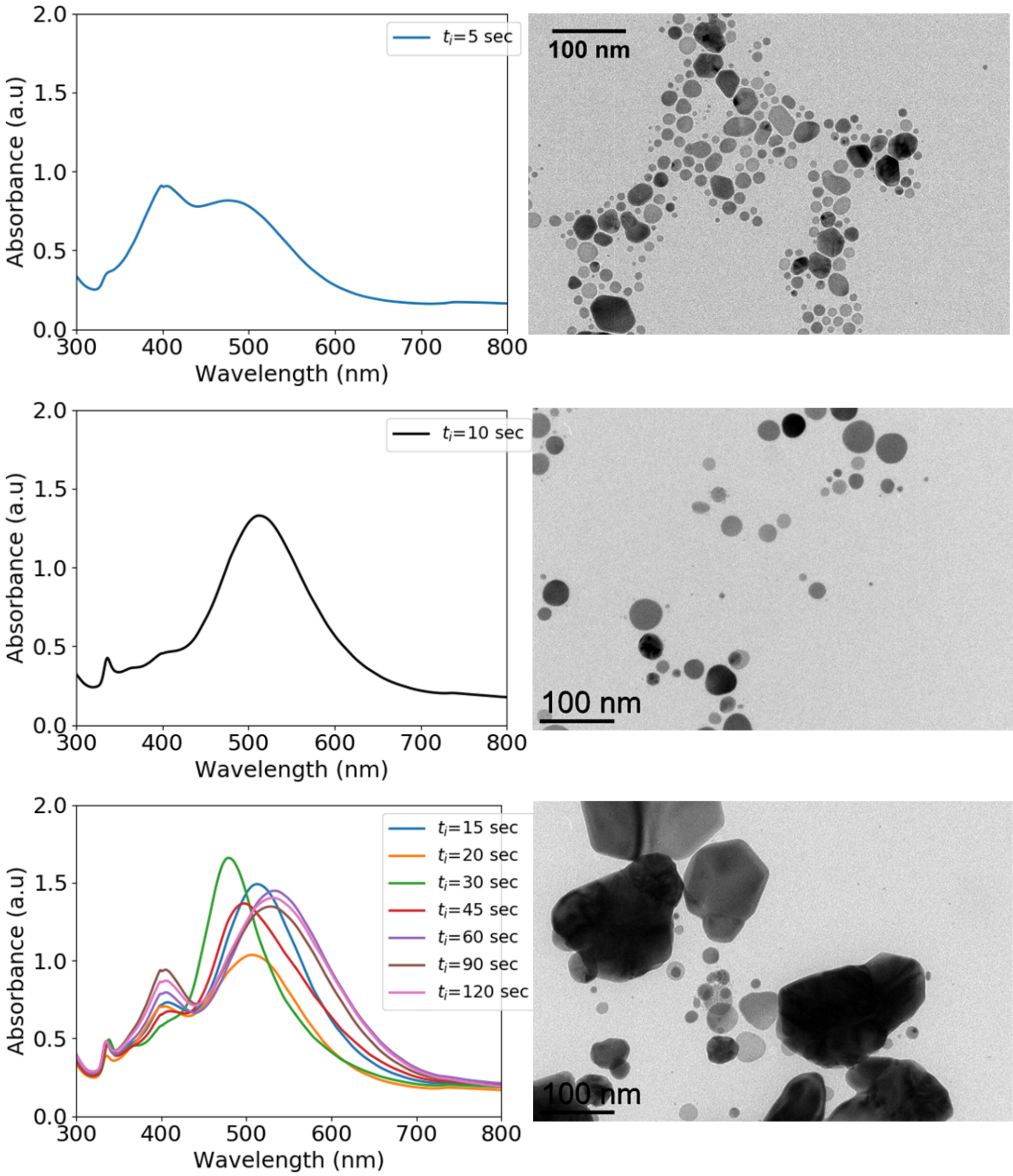

Figure 7: Influence of t_i on the synthesis at $10°C$.

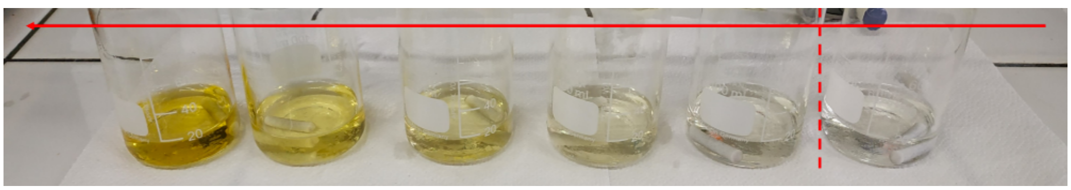

(a) 10°C

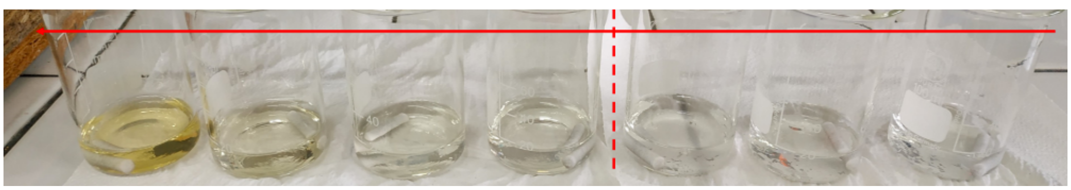

(b) 40°C

Figure 8: Results of the reduction of silver ions by $NaBH_4$ only for $NaBH_4$ concentrations equal to (from left to right): 1.49×10^{-3},7.45×10^{-4}, 3.64×10^{-4}, 1.91×10^{-4}, 9.36×10^{-5},4.68×10^{-5}, and 2.25×10^{-5} mM.